

2-D Lattice Flower Constellations for Radio Occultation Missions

Sanghyun Lee^{*1}, Daniele Mortari²

Department of Aerospace Engineering, Texas A&M University
College Station, Texas 77843-3141, USA

^{*1}kafalee@tamu.edu; ²mortari@tamu.edu

Abstract

This paper addresses the problem of designing suitable satellite constellations for Radio Occultation missions. Radio occultation for the Earth atmosphere usually requires global coverage and short interval measurements. The 2-D Lattice Flower Constellations theory is here applied to design constellations in order to maximize active time by providing global coverage with frequent measurements. Optimizations are performed using Genetic Algorithms to estimate constellation design parameters. Optimization is constrained by altitude range (to limit atmospheric drag and avoid Van Allen belts) while orbit nodal precession is used to obtain global coverage. The resulting constellation geometries have been explored from coverage performance perspective. Two coverage estimation methods have been used to evaluate coverage performances. Performances of some solutions are provided to make optimality selection.

Keywords

Radio Occultation Mission; Lattice Flower Constellations; Genetic Algorithms

Introduction

Radio Occultation (RO) is a recently proposed remote sensing technique to measure, in real time, physical parameters of the atmosphere, such as density and water vapor. The technique requires at least two satellites, one transmitting an electromagnetic signal and the other receiving it. The signal arriving to the receiver is refracted as it travels through the atmosphere, and the refraction magnitude is a function of the density and water vapor. Detailed information on radio occultation can be found in Ref. [Yunck 2002]. Since the GPS satellites have already provided this electromagnetic (radio) signal, techniques known as GPSRO are proposed for LEO satellites [Kursinski et al. 1997, Melbourne et al. 1994]. For GPSRO missions, the signal bending (due to the atmosphere refraction) is measured by detecting Doppler shift. In particular, it is possible to retrieve information on temperature and pressure using an

Abel transform [Bracewell 1965] for atmosphere altitudes below the ionosphere.

The name, *radio occultation*, comes from the odds for two satellites to see each other just before they are *occulted* by the Earth during the relative orbital motion. In that short time, when they can see each other through the atmosphere, the electromagnetic signal is sent and the radio occultation measurement can be performed. In general, for two satellites having different orbital periods, the RO measurement time happens only once per orbit. In this paper, we propose three different satellite constellations where a subset of satellite pairs sees each other for almost all the orbital period. In particular, these constellations, using circular orbits only, are analyzed and compared in terms of atmosphere coverage without consideration on the atmospheric refraction. When the actual atmospheric refraction is taken into account, the radius of the optimal orbit is slightly changed but the atmospheric coverage remains substantially identical.

When a radio signal from a transmitter passes through the atmosphere, its phase is perturbed in a way related to the atmospheric refractivity along the electromagnetic signal path. In general, the refraction angle is obtained from phase measurements on a receiver. Then, atmospheric quantities such as density, temperature, pressure, and moisture can be derived from it.

Radio Occultation missions can be classified into the following three categories:

1. two (or more) satellites on the same orbit (forming "string-of-pearls"),
2. geostationary satellites with Low Earth Orbit (LEO) satellites, and
3. Global Navigation Satellite System (GNSS) with LEO satellites [Liou et al. 2010].

The first RO experiment was performed during the occultation of the Mariner V spacecraft by Venus on 19

October 1967 after theoretical studies [Fjeldbo et al. 1965, 1971]. RO investigation using geostationary satellite with LEO satellite was made by radio link between two satellites in 1974 [Liu 1978]. The first was the Applications Technology Satellite (ATS-6) and the second was Geodetic Earth Orbiting Satellite (GEOS-3). Because these approaches provide limited data, many satellites are required for Earth's atmosphere global coverage, leading to unaffordable costs. This situation changed when Global Positioning System (GPS) signals were proposed to be used for RO. The RO technique has been applied to GPS signals as observed by LEO satellites in order to monitor the Earth's atmosphere with acceptable costs. The first experiment of GNSS-LEO was the GPS/MET (METeorology) experiment using the Microlab-1 satellite in 1995 [Melbourne et al. 1994, Ware et al. 1996]. Then, several other RO experiments have been conducted using GPS signals, notably CHAMP (Challenging Minisatellite Payload), GRACE (Gravity Recovery And Climate Experiment), and the FORMOSAT-3/COSMIC (Constellation Observing System for Meteorology, Ionosphere, and Climate) constellation [Wickert et al. 2001, Wickert et al. 2005]. Then, several RO missions using GNSS-LEO technique have been designed for the Russian GLONASS and the European Galileo constellations. With the advent of more efficient technologies, the use of cost-effective small satellites allows LEO-to-LEO links to provide global coverage with acceptable mission costs.

Optimal constellation design is a difficult problem because of the high dimensionality of the problem as each orbit depends on six parameters. However, it is possible to design different configurations of LEO satellites (LEO constellations) able to obtain high RO active times and global coverage. The optimal design of such constellations can be done using existing, well-proven, satellite constellation frameworks (e.g., Streets-of-coverage [Lüders 1961, Lüders et al. 1974] and Walker's [Walker 1971, 1974]) as well as the recently proposed 2-D Lattice Flower Constellations (LFC) [Avendaño et al. 2010]. The goal is to obtain a reasonable reduced problem dimensionality without cutting out potential useful solutions. For elliptical constellations, the LFC requires seven parameters three of which are integers; while for circular constellations, there are there integers in five parameters because eccentricity and argument of perigee are not necessary. The optimization of LFC implies that these five parameters have to be found to fulfill mission requirements. This research study

shows how to derive these parameters in order to maximize the atmosphere coverage. Reasonable initial radius ranges can be obtained by limiting the atmospheric drag and avoiding the inner Van Allen belt.

This paper is organized as follows. The first section of this paper briefly describes the radio occultation mission. Then, a summary on the 2-D LFC theory is provided. Then design considerations and parameters for LFC and optimize the design of the constellations are discussed. Finally, the performance of three selected constellations for radio occultation mission are presented.

Radio Occultation Mission

Mission Needs

The cost function defining the optimal RO constellation for global coverage of the Earth's atmosphere requires the maximization of the odds at which pairs of satellites can see each other through the atmosphere (active or observation time). In the next section, the basic geometry of two satellites is defined during the RO active time.

Geometry of Radio Occultation

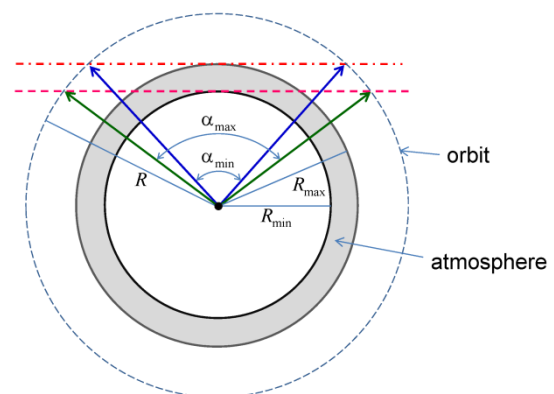


FIG. 1 TWO SATELLITE GEOMETRY DURING RADIO OCCULTATION ACTIVE TIME

The simplest optimal RO constellation is made of satellites on the same circular orbit of radius R . Fig.1 shows how the maximum central angle (α_{max}) between two satellites for RO mission depends on the minimum atmosphere radius (R_{min}) while minimum central angle (α_{min}) depends on maximum atmosphere radius (R_{max}). In this study we consider the atmosphere altitude ranging from 20 km to 200 km. Two satellites on the same circular orbit see each other through atmosphere if

$$\cos \alpha_{\max} \leq \frac{\mathbf{R}_i \cdot \mathbf{R}_j}{R^2} \leq \cos \alpha_{\min} \quad (1)$$

where $\alpha_{\max} = 2\cos^{-1}\left(\frac{R_{\min}}{R}\right)$, $\alpha_{\min} = 2\cos^{-1}\left(\frac{R_{\max}}{R}\right)$ and \mathbf{R}_i and \mathbf{R}_j are the position vectors of the i -th and the j -th satellite, respectively.

Atmosphere Coverage

1) Linear Swath Geometry of Two Satellites at a Specific Time

Linear swath between two satellites at a given instant time is as shown in Fig. 2. The satellites are located at orbital positions \mathbf{S}_i and \mathbf{S}_j , while the Earth's center is indicated by the point \mathbf{O} . The distance between the two satellites is L and the angles α and α^* are the central angles $\angle \mathbf{S}_i \mathbf{O} \mathbf{S}_j$ and $\angle \mathbf{S}_i^* \mathbf{O} \mathbf{S}_j^*$, respectively.

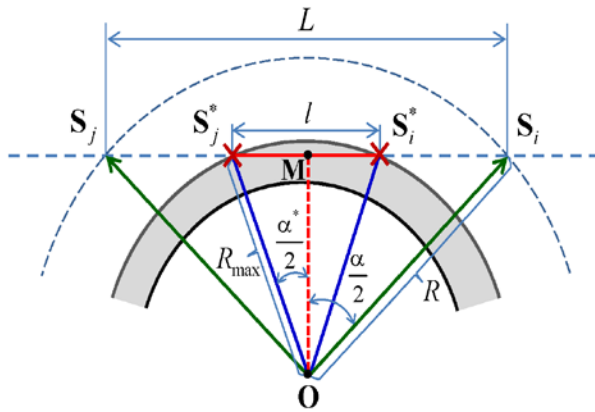


FIG. 2 LINEAR SWATH GEOMETRY FOR TWO SATELLITES AT A GIVEN TIME

To analyze the coverage, let us assume the radio signal is a line segment passing through the atmosphere with no refraction (which is practically very small). The end points of this segment are indicated by \mathbf{S}_i^* and \mathbf{S}_j^* , respectively. Midpoint of the segment is point \mathbf{M} . The length l of the linear swath is simply given by

$$l = 2R_{\max} \sin\left(\frac{\alpha^*}{2}\right) = 2R_{\max} \sqrt{1 - \cos^2\left(\frac{\alpha^*}{2}\right)} \quad (2)$$

where R_{\max} is maximum atmosphere height. Considering the two triangles, $\triangle \mathbf{O} \mathbf{M} \mathbf{S}_j^*$ and $\triangle \mathbf{O} \mathbf{M} \mathbf{S}_i^*$, we can write $\triangle \mathbf{O} \mathbf{M} \mathbf{S}_i^*$, we can write

$$\overline{\mathbf{O} \mathbf{M}} = R \cos\left(\frac{\alpha}{2}\right) = R_{\max} \cos\left(\frac{\alpha^*}{2}\right) \quad (3)$$

Then, using Eq. (3), we obtain

$$l = 2R_{\max} \sqrt{1 - \left[\frac{R}{R_{\max}} \cos\left(\frac{\alpha}{2}\right)\right]^2} = 2\sqrt{R_{\max}^2 - R^2 \frac{\cos \alpha + 1}{2}} \quad (4)$$

where R is orbital radius.

2) Planar Swath Geometry of Two Satellites During a Time Interval

Fig. 3 shows planar swath geometry for two satellites during a time step $(t_{k+1} - t_k)$. Considering two satellites in time t_k and t_{k+1} , we have 4 position vectors of satellites $[\mathbf{S}_i(t_k), \mathbf{S}_j(t_k), \mathbf{S}_j(t_{k+1}), \mathbf{S}_i(t_{k+1})]$.

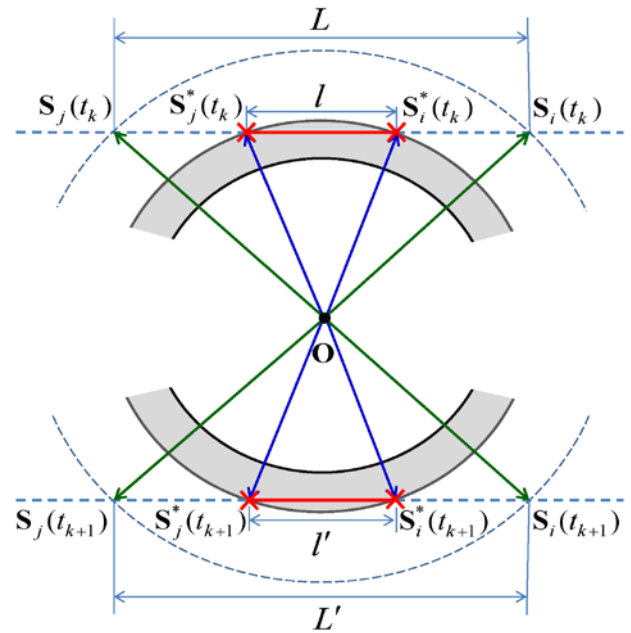


FIG. 3 PLANAR SWATH GEOMETRY FOR TWO SATELLITES DURING A TIME STEP

These position vectors indicate 4 vertices of planar swath that can be obtained as follows.

$$\begin{aligned} \mathbf{S}_i^*(t_k) &= \mathbf{S}_i(t_k) + \frac{\mathbf{S}_j(t_k) - \mathbf{S}_i(t_k)}{|\mathbf{S}_j(t_k) - \mathbf{S}_i(t_k)|} \frac{L-l}{2} \\ \mathbf{S}_j^*(t_k) &= \mathbf{S}_j(t_k) + \frac{\mathbf{S}_i(t_k) - \mathbf{S}_j(t_k)}{|\mathbf{S}_i(t_k) - \mathbf{S}_j(t_k)|} \frac{L-l}{2} \\ \mathbf{S}_i^*(t_{k+1}) &= \mathbf{S}_i(t_{k+1}) + \frac{\mathbf{S}_j(t_{k+1}) - \mathbf{S}_i(t_{k+1})}{|\mathbf{S}_j(t_{k+1}) - \mathbf{S}_i(t_{k+1})|} \frac{L'-l'}{2} \\ \mathbf{S}_j^*(t_{k+1}) &= \mathbf{S}_j(t_{k+1}) + \frac{\mathbf{S}_i(t_{k+1}) - \mathbf{S}_j(t_{k+1})}{|\mathbf{S}_i(t_{k+1}) - \mathbf{S}_j(t_{k+1})|} \frac{L'-l'}{2} \end{aligned} \quad (5)$$

These 4 points, $[\mathbf{S}_i^*(t_k), \mathbf{S}_j^*(t_k), \mathbf{S}_i^*(t_{k+1}), \mathbf{S}_j^*(t_{k+1})]$, identify a quadrilateral planar swath. The time step is small enough to assume that satellites move in straight line. Since this quadrilateral is skew, these points are transformed to topocentric-horizontal

coordinate system with projection to surface.

3) First Coverage Estimation-sum of Areas of Simple and Complex Quadrilaterals

There are two quadrilateral cases as shown in Fig. 4. The first one is simple quadrilateral while the other is a complex (self-intersecting) quadrilateral.

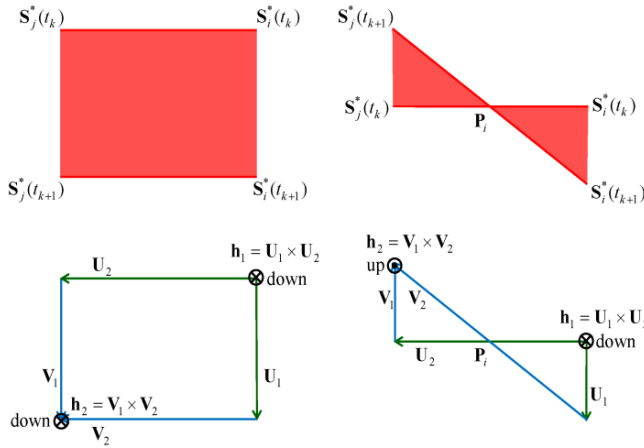


FIG. 4 SIMPLE AND COMPLEX QUADRILATERALS

Using position vectors which are given by Eq. (5) we can get vectors such as U_1 , U_2 , V_1 and V_2 . Then, vectors h_1 and h_2 can be obtained by cross products as shown in Fig. 4. The condition associated with a simple quadrilateral is

$$h_1 \cdot h_2 > 0 \quad (6)$$

Because all quadrilaterals consist of two triangles regardless of shape, area of simple or complex quadrilaterals can always be obtained by summing the areas of two triangles. Area for simple case is obtained by

$$A_{\text{simple}} = \frac{|h_1|}{2} + \frac{|h_2|}{2} \quad (7)$$

In complex case, there are some additional processes because we find intersecting point (P_i) and then define related vectors as follows.

$$\begin{aligned} U_2' &= P_i - S_i^*(t_k) \\ V_2' &= S_j^*(t_k) - P_i \\ h_1' &= U_1 \times U_2' \\ h_2' &= V_1 \times V_2' \end{aligned} \quad (8)$$

Similarly, area for complex case is given by

$$A_{\text{complex}} = \frac{|h_1'|}{2} + \frac{|h_2'|}{2} \quad (9)$$

The total coverage is obtained by summing all planar swaths by all satellites pairs combinations. For instance, by summing all planar swaths by all

satellite combinations during one quart of the period gives a quarter period coverage. However, net coverage cannot be obtained this way because of the existing overlapping areas. In order to estimate the net coverage, methods to count overlapping area are required.

4) Second Coverage Estimation - Using Uniform Distributed Points on a Sphere

The creation of uniform distribution of points on a sphere can be used to estimate net coverage by checking the number of overlapping times. Among all the existing methods to generate uniformly distributed points on a sphere the method presented in Ref. [Mortari et al. 2011] is adopted here. Starting with an icosahedron (20 identical equilateral triangular faces) and performing 8 sequential divisions in identical spherical triangles, $20 \cdot 2^8 = 5,120$ triangles with same spherical areas are obtained whose centers approximate 5,120 uniformly distributed points on a sphere, as shown in Fig. 5.

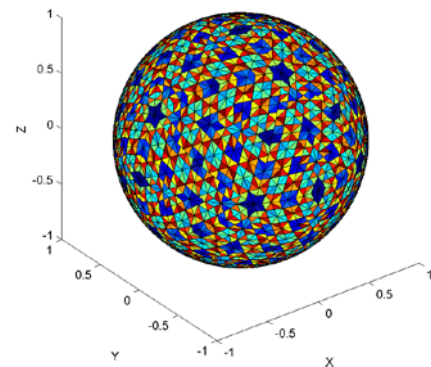


FIG. 5 ICOSAHDEN SPLIT BY 8 DIVISIONS

Because every planar swath is quadrilateral, it can be divided into two triangles. Therefore, checking if points are inside or outside triangle can determine if points are observed or not. Fig. 6 shows the geometry of observation and non-observation cases. In case of observation (left), the sum of the areas of the three sub-triangles is equal to the area of the original triangle while the non-observation case (right) is experienced if the total area is greater than the area of the original triangle.

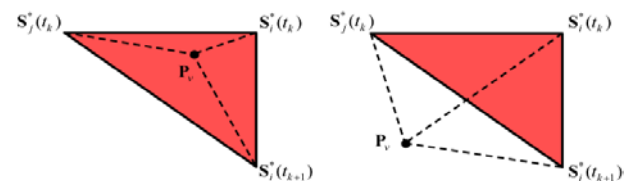


FIG. 6 GEOMETRY OF OBSERVATION AND NON-OBSERVATION CASES

In order to check observation condition, all uniformly distributed points are transformed to topocentric-horizon coordinate system with mid-point of triangle as origin, and then projected to surface as all points of quadrilateral are transformed. Equation to check whether the point P_v is observed is given by.

$$A(\mathbf{P}_v \mathbf{S}_i^*(t_k) \mathbf{S}_j^*(t_k)) + A(\mathbf{P}_v \mathbf{S}_j^*(t_k) \mathbf{S}_i^*(t_{k+1})) + A(\mathbf{P}_v \mathbf{S}_i^*(t_{k+1}) \mathbf{S}_j^*(t_k)) = A(\mathbf{S}_i^*(t_k) \mathbf{S}_j^*(t_k) \mathbf{S}_i^*(t_{k+1})) \quad (10)$$

2-D Lattice Flower Constellations Design

The 2-D Lattice Flower Constellations (LFC) design methodology has been introduced in Ref. [16]. In general LFC are characterized by four continuous parameters (semi-major axis, eccentricity, inclination and argument of perigee) and three independent integer parameters establishing the constellation satellite distribution in the (M, Ω) -space. These integer parameters are: the number of orbital planes, N_o , the number of satellites per orbit, N_{so} , and the configuration number, N_c (phasing parameter). Using these integer parameters the satellites' right ascension of the ascending node (Ω_{ij}) and the initial mean anomaly (M_{ij}) are solutions of the following equation

$$\begin{bmatrix} N_o & 0 \\ N_c & N_{so} \end{bmatrix} \begin{Bmatrix} \Omega_{ij} \\ M_{ij} \end{Bmatrix} = 2\pi \begin{Bmatrix} i-1 \\ j-1 \end{Bmatrix} \quad (11)$$

where $i = 1, \dots, N_o$, $j = 1, \dots, N_{so}$, and $N_c \in [1, N_o]$. The " $i-j$ " element is the j -th satellite on the i -th orbital plane. If repeating ground tracks are required, then the compatibility equation

$$N_p T_p = N_p \frac{2\pi}{n + \dot{\omega}} = N_d T_d = N_d \frac{2\pi}{\omega_{\odot} - \dot{\Omega}}, \quad (12)$$

where T_p is the orbit nodal period and T_d is the Greenwich nodal period, provides the value of the orbit radius for each coprime integers, N_p and N_d . Eq. (12) takes into account the main gravitational perturbation due to the Earth oblateness, known as the J_2 effect. The secular and persistent J_2 effect modifies the mean motion according to

$$n = n_0 \left[1 + \frac{3}{4} J_2 \left(\frac{R_{\oplus}}{p} \right)^2 (2 - 3 \sin^2 i) \sqrt{1 - e^2} \right], \quad (13)$$

where $n_0 = \sqrt{\frac{\mu}{a^3}}$ is the unperturbed mean motion, linearly changes the right ascension of the ascending

node,

$$\dot{\Omega} = -\frac{3}{2} J_2 \left(\frac{R_{\oplus}}{p} \right)^2 n \cos i, \quad (14)$$

as well as the argument of perigee,

$$\dot{\omega} = \frac{3}{4} J_2 \left(\frac{R_{\oplus}}{p} \right)^2 n (5 \cos^2 i - 1). \quad (15)$$

The LFC theory allows us to design constellations using circular or small eccentric orbits, within the range of validity of Carter's definition of compatibility, given in Eq. (12). For non small eccentric orbits, the J_2 perturbation slowly destroys the constellation if no control is used to compensate the rotation of the apse line. However, in this paper circular orbits will be adopted, therefore, we can set $e=0$ while ω (not defined for circular orbits) can be set to any constant value. Then, the number of continuous parameters for LFC is reduced from 4 to 2. In addition, all satellites in the constellation have same semi-major axis and inclination in order to avoid different orbital nodal regression.

Minimum Distance Constraint

To avoid the design of constellations with satellites colliding the results provided by Ref. [Speckman et al. 1990] is adopted. In that analytical study, the closest approach between the two satellites (ρ_{\min}) in two circular orbits with the same radius and inclination, is analytically expressed by the following equation

$$\rho_{\min} = 2 \sqrt{\frac{1 + \cos^2 i + \sin^2 i \cos \Delta\Omega}{2}} \sin \left(\frac{\Delta F}{2} \right) \quad (16)$$

Where

$$\Delta F = \Delta M - 2 \tan^{-1} \left[-\cos i \tan \left(\frac{\Delta\Omega}{2} \right) \right]$$

and where ΔM and $\Delta\Omega$ are the differences in mean anomaly and right ascension of ascending node, respectively. Note that ρ_{\min} must be scaled by the orbit radius to find the actual value of the minimum approach distance. Due to the regular pattern (lattice) of the LFC, it is not necessary to evaluate the minimum distance using all pairs of satellites. It is sufficient to evaluate the minimum distance between the first satellite $[\Omega_{11}, M_{11}]$ with all the other satellites staying on different orbital planes. This greatly simplifies the effort in the optimization to avoid constellations affected by satellite conjunctions

(sometime common for symmetric distribution). Constraint that no two satellites are ever closer than half the distance between two consecutive satellites in the same orbit has been used. For the specific case of $N_{so} = 1$ (just one satellite per orbit), the constraint adopted is that the minimum distance between any pair of satellites is greater than 100 km.

LFC Optimization

1) Genetic Algorithms

Genetic Algorithms are empirical methods to solving optimization problems by mimic the natural selection/mutation process driving the biological evolution. More information about Genetic Algorithms is available in Ref. [Goldberg 1989]. Although there is no guarantee that Genetic Algorithms provide the optimal solution (and this is true for most optimization methods), Genetic Algorithms are most suited in multi-parameter and highly nonlinear problems [Gallagher et al. 1994]. Because constellation design for radio occultation is a highly nonlinear problem, a Genetic Algorithm has been selected to find the optimal constellation parameters for the given set of mission requirements.

2) Fitness Function

The fitness function utilized to drive the optimization process is designed to maximize the percentage of active time with respect to a reference time. Fitness function has been implemented to count the times that pairs of satellites see each other through the atmosphere. This is simply determined by the geometric conditions expressed by Eq. (1). For computation of the percentage of active time, geometric conditions for all the $i-j$ satellite combinations should be considered. Thus, the optimality is defined by the minimization of the following function

$$L = \left(\frac{K \Delta t}{T} \right)^{-1} \quad (17)$$

where K is the number of times satisfying geometric conditions, Δt is the time step, and T is the orbital period.

3) Design Parameter Constraints

In order to run the optimization process the design space should be first defined. Acceptable orbit radius is bounded by the maximum atmosphere

altitude (to limit the atmospheric drag) and by the inner Van Allen radiation belt. The maximum altitude is set to $h_{\max} = 1,000$ km because the lower boundary of the inner Van Allen Radiation belt is located at an altitude of about 1,000 km [Gilmore 2002]. Considering atmospheric drag, the minimum altitude is set to $h_{\min} = 300$ km. Lower altitude are impractical due to the larger atmospheric drag [Young et al. 2000]. Using these two altitude constraints the maximum and minimum periods are

$$T_{\min} = 2\pi \sqrt{\frac{(R_{\oplus} + h_{\min})^3}{\mu}} \quad \text{and} \quad T_{\max} = 2\pi \sqrt{\frac{(R_{\oplus} + h_{\max})^3}{\mu}},$$

where R_{\oplus} and μ are the Earth's radius and gravitational constant, respectively. The ranges of these parameters are given in Table 1.

TABLE 1 PARAMETERS RANGE

Parameters	Range
$[N_o, N_{so}]$	$[1,12] [2,6] [3,4] [4,3] [6,2] [12,1]$
N_c	$[1, N_o]$
T	$[1.51 \text{ hr}, 1.75 \text{ hr}]$
i	$[0, 180 \text{ deg}]$

Re-oriented Constellation

Any constellation can be re-oriented just by using rigid rotation matrix with free selection of axis and angle of rotation in order to provide desired performance in specific region. In Fig. 7, \hat{n}_k , \hat{e}_k and \hat{h}_k are node, eccentricity, and angular momentum vectors of k -th orbit in the constellation, respectively.

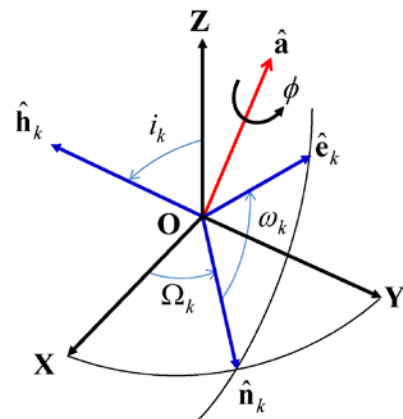


FIG. 7 RIGID ROTATION MATRIX WITH FREE SELECTION OF AXIS AND ANGLE OF ROTATION

Node vector and eccentricity vector of each orbit in the constellation can be expressed in terms of orbit elements as follows.

$$\begin{aligned}\hat{\mathbf{h}}_k &= f_1(i_k, \Omega_k) \\ \hat{\mathbf{e}}_k &= f_2(i_k, \Omega_k, \omega_k)\end{aligned}\quad (18)$$

where i_k , Ω_k , ω_k are the inclination, the right ascension of the ascending node and the argument of perigee of k -th orbit, respectively. Then, considering rotating-plane lattice flower constellations with circular orbits and same orbit inclination, we obtain

$$\begin{aligned}\hat{\mathbf{h}}_k &= f_1(i, \Omega_k) \\ \hat{\mathbf{e}}_k &= f_2(i, \Omega_k)\end{aligned}\quad (19)$$

Rigid rotation matrix is given by

$$\mathbf{R}(\hat{\mathbf{a}}, \phi) = I_{3 \times 3} \cos \phi + (1 - \cos \phi) \hat{\mathbf{a}} \hat{\mathbf{a}}^T + [\hat{\mathbf{a}} \times] \sin \phi \quad (20)$$

where $\hat{\mathbf{a}}$ and ϕ are axis and angle of rotation, respectively [Schaub et al. 2009].

Using the rigid rotation matrix, angular momentum and eccentricity vectors can be obtained as follows

$$\begin{aligned}\hat{\mathbf{h}}'_k &= \mathbf{R}(\hat{\mathbf{a}}, \phi) \hat{\mathbf{h}}_k = g_1(i'_k, \Omega'_k) \\ \hat{\mathbf{e}}'_k &= \mathbf{R}(\hat{\mathbf{a}}, \phi) \hat{\mathbf{e}}_k = g_2(i'_k, \Omega'_k)\end{aligned}\quad (21)$$

Results

Optimal Radio Occultation Constellations

1) String-of-pearls Polar Constellation

The first constellation analyzed for radio occultation mission is a single-orbit, conventional, string-of-pearls constellation whose design parameters are given in Table 2. There is no single unique optimal solution because inclination i is independent of the active time when there is one orbital plane in constellation. In order to provide global coverage the orbit inclination is set to 90° (polar orbit).

TABLE 2 LFC PARAMETERS OF STRING-OF-PEARLS POLAR CONSTELLATION

Parameters	Optimal Values
$[N_o, N_{so}]$	[1,12]
N_c	N_o
T	1.51 (hr)
i	90 (deg)

Fig. 8 illustrates the satellite trajectories of the string-of-pearls polar constellation as seen from the Earth-Centered Inertial (ECI) frame. All satellites of this constellation have same orbital plane and all two consecutive satellites see each other, as shown in the figure. This polar orbit constellation provides

global coverage due to the rotation of the Earth. However, long time is required to complete the global coverage and the coverage density is strongly latitudinal dependent with maximum observation at poles.

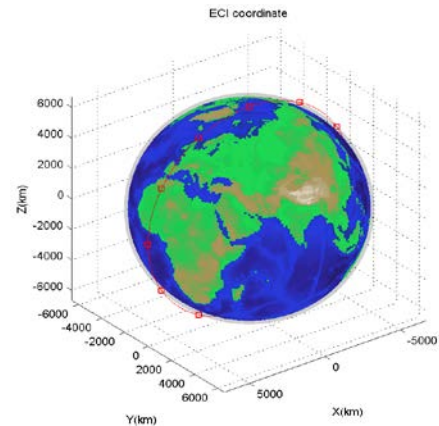


FIG. 8 STRING-OF-PEARLS POLAR CONSTELLATION

2) Plane Lattice Flower Constellations

Although all satellites of a constellation don't have same orbital plane, it is possible to design constellations whose satellites lie on the same plane using different orbital planes. Compared with conventional string-of-pearls polar constellation, these constellations have advantage of relatively short time to cover global area although they can not provide global coverage. The disadvantage is that the deployment of this constellation may require more than a single launch. These constellations are called *plane lattice flower constellations*. The LFC parameters of designed plane lattice flower constellations are provided in Table 3. First one is called *rotating-plane lattice flower constellation* because axis of plane is coning about a fixed axis. The other is called *fixed-plane lattice flower constellation* because the plane where the satellites do not change its orientation.

TABLE 3 LFC PARAMETERS OF PLANE LATTICE FLOWER CONSTELLATION

Parameters	Rotating-plane LFC	Fixed-plane LFC
$[N_o, N_{so}]$	[6,2]	[12,1]
N_c	1	0
T	1.51 (hr)	1.51 (hr)
i	21.78 (deg)	76.94 (deg)

Figs. 9 - 10 show the satellite trajectories of plane lattice flower constellations as seen from the ECI frame.

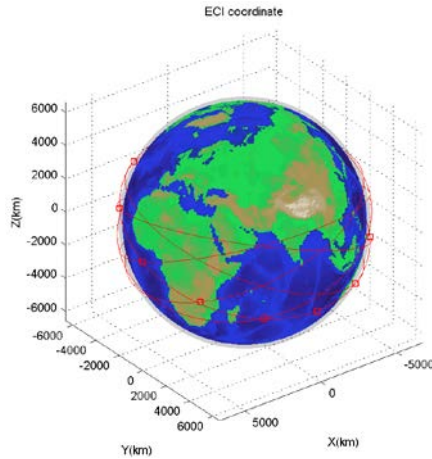


FIG. 9 ROTATING-PLANE LATTICE FLOWER CONSTELLATION

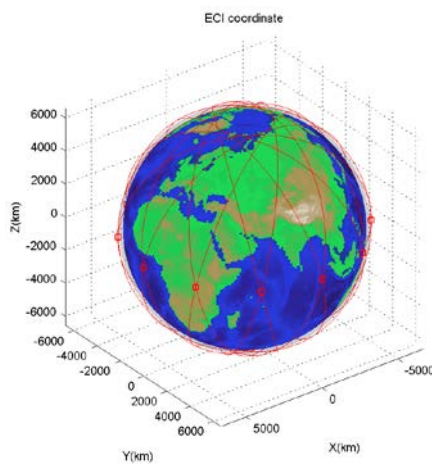


FIG. 10 FIXED-PLANE LATTICE FLOWER CONSTELLATION

When all satellites of a constellation lie in the same plane, then the rank of a matrix made of the position vectors must be 2. This position matrix is given by Eq. (22).

$$\mathbf{M} = [\hat{\mathbf{r}}_1 \quad \hat{\mathbf{r}}_2 \quad \cdots \quad \hat{\mathbf{r}}_n] \quad (22)$$

where n is the total number of satellites. Since the rank of a matrix is equal to the number of non-zero singular values, the singular values of a quadratic form of the matrix have been computed.

Minimum singular values of the position matrix for various inclinations, $[N_o, N_{so}, N_c] = [6, 2, 1]$ and $T = 1.51$ (hr) are shown in Fig. 11 for the rotating-plane LFC. The rotating-plane LFC is really planar for low inclinations. Of course, for fixed-plane LFC, the rank of the position matrix is always 2, as we expected.

Note that, using designed conditions, rotating-plane LFC can be used for low inclinations. In case of fixed-plane LFC, minimum singular values for various inclinations are always zero.

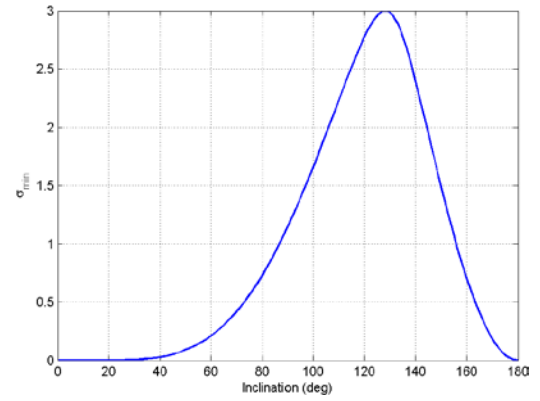


FIG. 11 MINIMUM SINGULAR VALUES FOR VARIOUS INCLINATIONS, $[N_o, N_{so}] = [6, 2]$, $N_c = 1$ and $T = 1.51$ (hr) IN ROTATING-PLANE LFC

Two Coverage Performance Evaluations

1) First Coverage Estimation Result- sum of Areas of Simple and Complex Quadrilaterals

In this simulation, we set a time step to $\frac{T}{100}$.

Single planar swath by two satellite of rotating-plane lattice flower constellation with single time step is displayed in Fig. 12. Quarter period coverage can be estimated by summing all planar swaths by all satellite combinations during a quarter period. However, the estimated coverage is not net coverage because there are overlapping areas as shown in Fig. 13.

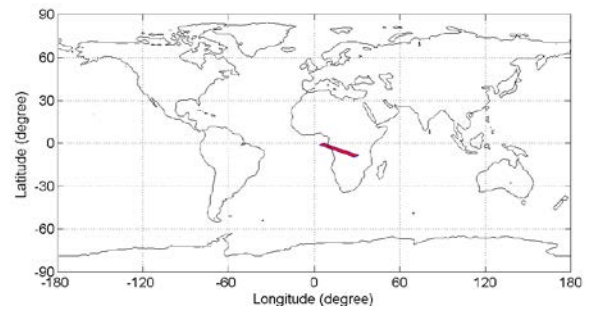


FIG. 12 SINGLE PLANAR SWATH BY TWO SATELLITES WITH SINGLE TIME STEP

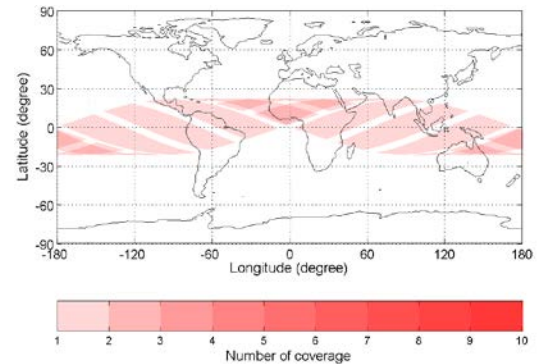


FIG. 13 A QUARTER PERIOD COVERAGE OF ROTATING-PLANE LATTICE FLOWER CONSTELLATION

2) Second Coverage Estimation Result- Using Uniform Distributed Points on a Sphere

In order to verify method using uniform distribution of point on a sphere, total coverage are estimated using various number of uniform distributed points on a sphere. Single period coverage percent and errors obtained with different number of points on string-of-pearls polar constellation are in Table 4. Because single planar swath of string-of-pearls polar constellation is narrower than other constellations, two coverage estimation methods have most significant difference in this constellation. Therefore, two coverage estimation methods are applied to string-of-pearls polar constellation. Errors are calculated by comparing with result which is obtained by sum of quadrilaterals (8.64%).

TABLE 4 COMPARISON OF TOTAL COVERAGE OBTAINED WITH DIFFERENT NUMBER OF POINTS

Number of Points	Total Coverage (%)	Error (%)
2,560	15.24	76.4
5,120	11.56	33.8
10,240	9.65	11.7
20,480	8.96	3.7
81,920	8.86	2.6
163,840	8.67	0.3
1,310,720	8.65	0.1

From these results, we can conclude that method using uniform distribution of point on a sphere needs appropriate number of points to give accurate results. Simulation with 1,310,720 points was performed in order to estimate net coverage. Single period simulation results of all designed constellations are shown in Figs. 14-16. Results by uniform distribution of point on a sphere are shown in Earth-Centered Earth-Fixed (ECEF) frame and have good agreement with 2D-view results of first coverage estimation method.

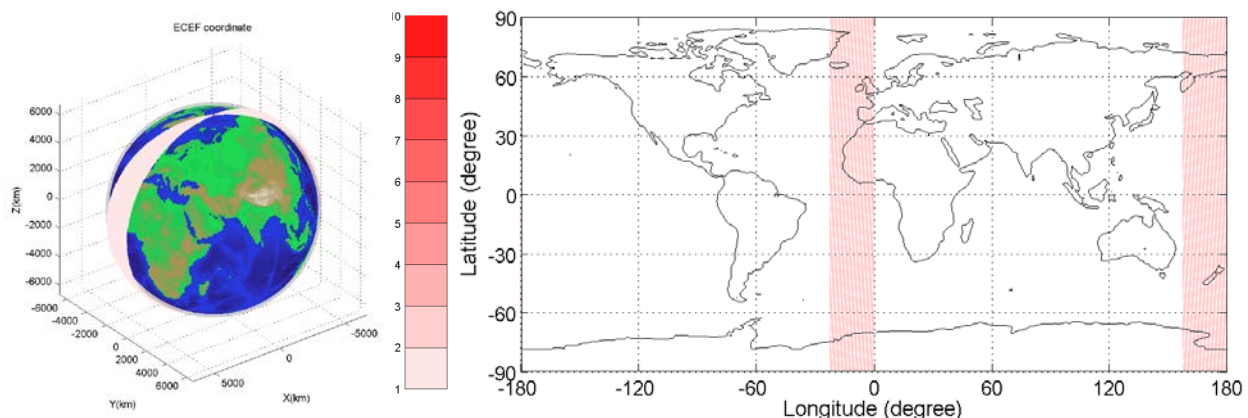


FIG. 14 SINGLE PERIOD COVERAGE OF STRING-OF-PEARLS POLAR CONSTELLATION

3) Comparison of Coverage Performances

As mentioned above, net coverage can be obtained by method with uniform distribution of points in sphere. Comparison of coverage performances by designed constellations are provided in Table 5. Plane lattice flower constellations provides global coverage with relatively short time while string-of-pearls polar constellation require long time to cover global area. As shown in Fig. 15 and Fig. 16, rotating-plane lattice flower constellation provide good performance in a low latitude region while fixed-plane lattice flower constellation is suitable in a high latitude region.

TABLE 5 COMPARISON OF COVERAGE PERFORMANCES (NET COVERAGE, %)

Time	String-of-pearls Polar	Rotating-plane LFC	Fixed-plane LFC
1 period	8.63	36.20	77.27
0.5 day	68.95	36.90	87.87
1 day	90.32	36.92	88.09

Re-oriented Rotating-Plane Lattice Flower Constellations

Using the relationship Eq. 21, we obtain orbit elements of the re-oriented constellation. Note that, re-oriented constellation has different inclination while original plane lattice flower constellation has identical inclination.

Figs. 17 and 18 show the satellite trajectories and single period coverage of the re-oriented plane lattice flower constellations. Note that the re-oriented plane lattice flower constellations provide service in specific regions. The re-oriented fixed-plane flower constellation provides good performance in mid latitudes areas including highly populated regions such as the United States, Europe and Northeast Asia.

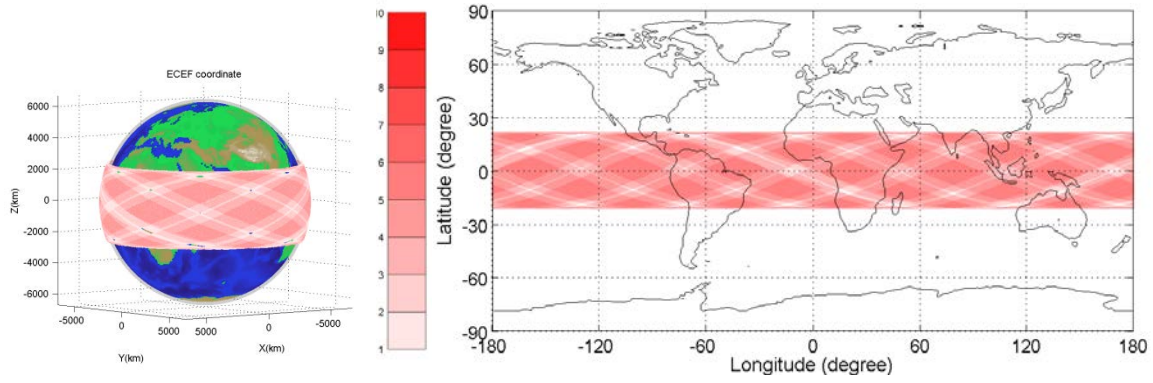


FIG. 15 SINGLE PERIOD COVERAGE OF ROTATING-PLANE LATTICE FLOWER CONSTELLATION

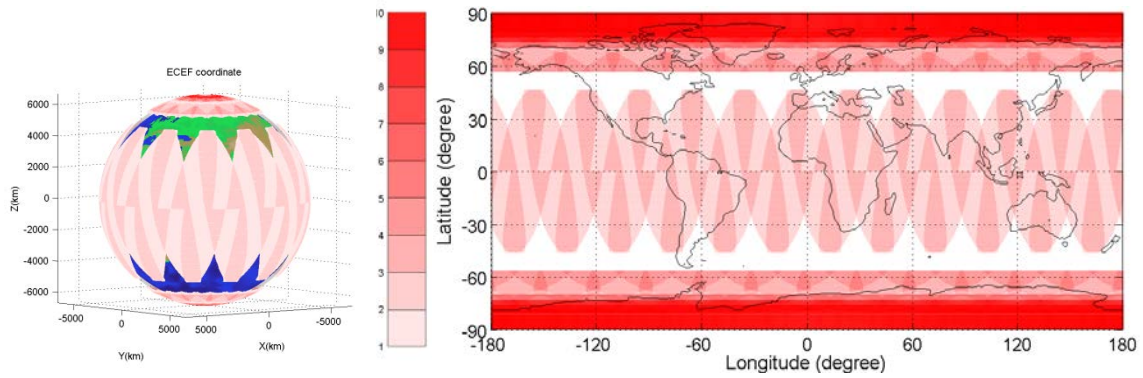


FIG. 16 SINGLE PERIOD COVERAGE OF FIXED-PLANE LATTICE FLOWER CONSTELLATION

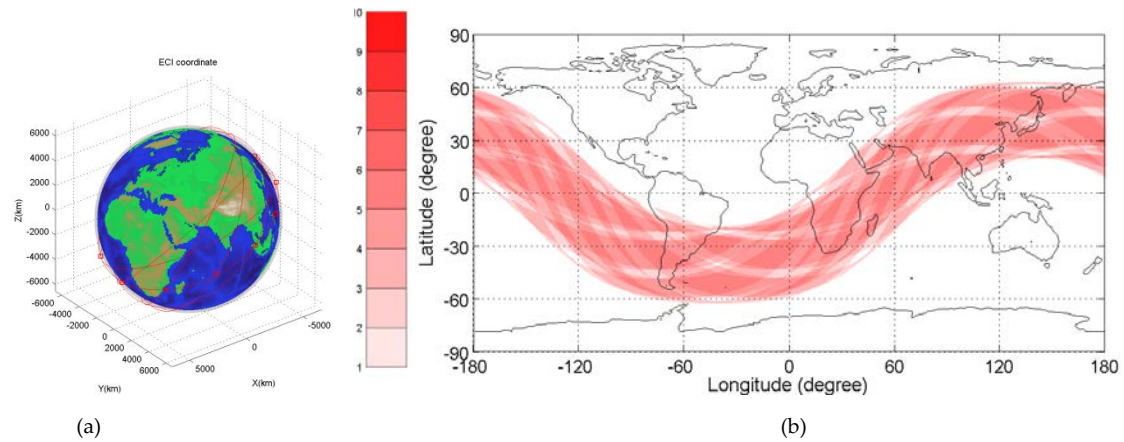


FIG. 17 RE-ORIENTED ROTATING-PLANE LATTICE FLOWER CONSTELLATION (a) THE SATELLITE TRAJECTORIES (b) SINGLE PERIOD COVERAGE IN 2D-VIEW

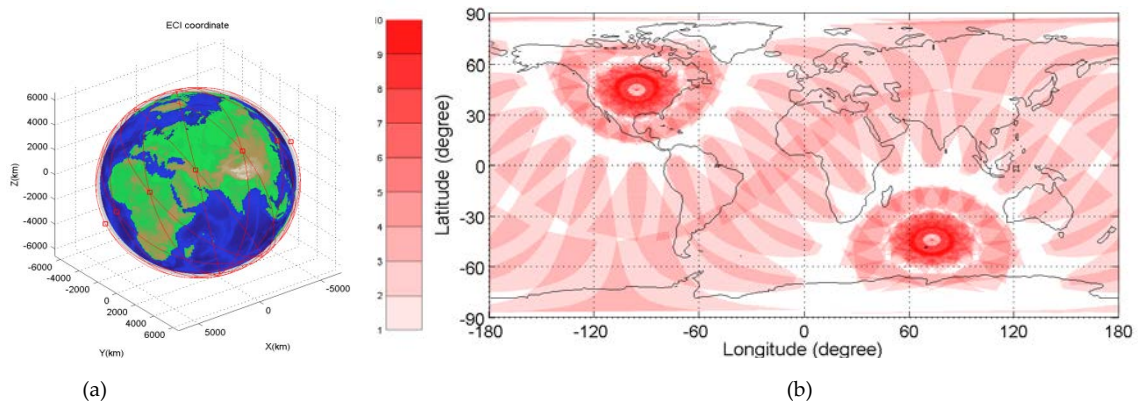


FIG. 18 RE-ORIENTED FIXED-PLANE LATTICE FLOWER CONSTELLATION (a) THE SATELLITE TRAJECTORIES (b) SINGLE PERIOD COVERAGE IN 2D-VIEW

Conclusions

In this work, we analyzed and designed constellations for radio occultation mission of the Earth atmosphere. The Genetic Algorithms technique with 2-D Lattice Flower Constellation theory has been used to find the best constellation for the mission. Three different satellite constellations are found by maximizing active time with minimum distance constraint. Optimal solutions have not only conventional string-of-pearls polar constellation but also novel plane lattice flower constellation which have good coverage characteristics. In order to evaluate coverage performance, geometries of linear and planar swaths have been investigated and total coverage has been estimated. To count overlapping areas, uniform distribution of points on a sphere is introduced and net coverage of three different satellite constellations have been estimated by checking observation conditions of all uniformly distributed points on the sphere. It has been found that the proposed plane lattice flower constellations provide good performance for time to cover global area although they can't provide coverage for entire Earth. The rotating-plane lattice flower constellation and the fixed-plane lattice flower constellation have good coverage characteristics in low and high latitude region, respectively. In addition, the re-oriented plane lattice flower constellations provide good coverage performance in specific regions.

REFERENCES

- Avendaño, M., Mortari, D., and Davis, J. J. "The Lattice Theory of Flower Constellations." 20th AAS/AIAA Space Flight Mechanics Meeting, San Diego, California, February 14-18, 2010.
- Bracewell, Ronald. The Fourier Transform and its Applications, McGraw-Hill, 1965.
- Fjeldbo, Gunnar and Eshleman, V. R. "The Bistatic Radar Occultation Method for the Study of Planetary Atmosphere." Journal of Geophysical Research, vol. 70, no. 13 (1965):3217-3225.
- Fjeldbo, Gunnar and Kliore, Arvydas J. "The Neutral Atmosphere of Venus as Studied with the Mariner V Radio Occultation Experiments." Astronomical Journal, vol. 76, no. 2 (1971): 123-140.
- Gallagher, K. and Sambridge, M. "Genetic Algorithms: A Powerful Tool for Large-scale Nonlinear Optimization Problems." Computers & Geosciences, vol. 20, no. 7/8 (1994): 1229-1236.
- Gilmore, D. G. Spacecraft Thermal Control Handbook. Volume I: Fundamental Technologies. Reston, Virginia: The Aerospace Corporation, 2002.
- Goldberg, D. E. Genetic Algorithms in Search, Optimization and Machine Learning. Boston, Massachusetts: Addison- Wesley Longman Publishing Co., Inc., 1989.
- Kursinski, E. R., Haji, G. A., Schofield, J. T., Linfield, R. P., and Hardy, K. R. "Observing Earth's Atmosphere by Occultation Using Global Positioning System." Journal of Geophysical Research, vol. 102, no. 19 (1997): 23,429-23,465.
- Liou, Y. A., Pavelyev, A. G., Matyugov, S. S., Yakovlev, O. I., Wickert, J. Radio Occultation Method for Remote Sensing of the Atmosphere and Ionosphere. Vokovar, Croatia :Intech, 2010.
- Liu, Anthony S. "On the Determination and Investigation of the Terrestrial Ionospheric Refractive Indices using GEOS-3/ATS-6 Satellite-to-Satellite Tracking Data." Radio Science, vol. 13, no. 2 (1978): 709-716.
- Lüders, R. D. "Satellite Networks for Continuous Zonal Coverage." American Rocket Society Journal, vol. 31 (1961): 179-184.
- Melbourne, William et al., "The Application of Spaceborne GPS to Atmospheric Limb Sounding and Global Change Monitoring." Pasadena, California: National Aeronautics and Space Administration, Jet Propulsion Laboratory, California Institute of Technology, 1994.
- Mortari, D., Avendaño, M. and Davalos, P. "Uniform Distribution of Points on a Sphere with Application in Aerospace Engineering." 20th AAS/AIAA Space Flight Mechanics Meeting, New Orleans, Louisiana, February 13-17, 2011.
- Schaub, H. and Junkins, J. L. Analytical Mechanics of Space Systems. Reston, VA: American Institute of American and Astronautics, 2009.
- Speckman, L. E., Lang, T. J., and Boyce, W. H. "An Analysis of the Line of Sight Vector Between Two Satellites in Common Altitude Circular Orbits." Proceedings of AIAA/AAS Astrodynamics Conference, Portland, Oregon, August 20-22, 1990.

- Walker, J. G. "Some Circular Orbit Patterns Providing Continuous Whole Earth Coverage." *British Interplanetary Journal Society*, vol. 24 (1971): 369–384.
- Walker, J.G. "Continuous Whole-Earth Coverage by Circular Orbit Satellite Patterns." Tech. Rep. 77044, Royal Aircraft Establishment, 1977.
- Ware, R., et al., "GPS Sounding of the Atmosphere from Low Earth Orbit: Preliminary Results." *Bulletin of the American Meteorological Society*, vol. 77, no. 1 (1996): 19-40.
- Wickert, Jens et al., "Atmosphere Sounding by GPS Radio Occultation: First Results from CHAMP." *Geophysical Research Letters*, vol. 28, no. 17 (2001): 3263-3266.
- Wickert, Jens et al. "GPS Radio Occultation with CHAMP and GRACE: A First Look at a New and Promising Satellite Configuration for Global Atmospheric Sounding." *Annales Geophysicae*, vol. 23 (2005): 653-658.
- Young, M., Muntz, E., and Wang, J. "Maintaining Continuous Low Orbit Flight by Using In-Situ Atmospheric Gases for Propellant." *Rarefied Gas Dynamics: 22-nd International Symposium*, Sydney, Australia, July 9–14 2000.
- Yunck, Thomas P. "An Overview of Atmospheric Radio Occultation." *Journal of Global Positioning Systems*, vol. 1, no. 1 (2002): 58-60.